Available online at www.sciencedirect.com
SCIENCE DIRECT
International Journal of Heat and Mass Transfer 49 (2006) 2277–2290
International Journal of HEAT and MASS TRANSFER
www.elsevier.com/locate/ijhmt

Mathematical models based on heat transfer and coupled heat and mass transfers for rapid high temperature treatment in fluidized bed: Application for grain heat disinfestation

T. Madhiyanon [a,*], A. Techaprasan [b], S. Soponronnarit [b]

[a] Department of Mechanical Engineering, Mahanakorn University of Technology, Bangkok 10530, Thailand
[b] School of Energy and Materials, King Mongkut's University of Technology, Thonburi, Bangkok 10140, Thailand

Received 28 September 2004
Available online 9 March 2006

Abstract

This study sought to develop a mathematical model of rapid, high temperature heat treatment of stored grains in a fluidized bed. The model was intended to evaluate dynamic changes in temperature distributions inside grain kernel, and grain and exit air temperatures. No differences in temperature profiles within individual paddy kernels obtained from either analytical or numerical solutions for one- and two-dimensional heat diffusion models were found. Cylindrical coordinates gave clearer pictures of temperature profiles than spherical coordinates, and the former was chosen for the model. Thin-layer heat diffusion alone is inadequate for explaining transport phenomena in a fluidized bed; it must be incorporated into a deep bed model. The loss of as little as 1.0% dry basis moisture content from the grain surface during heating significantly affected the predictiveness of the model. Therefore, a model coupling heat and mass transfer performs much better in predicting grain and exit air temperatures than one that neglects the effect of moisture loss, when compared with the experimental results. The results showed agreement between the measured and predicted results, although the predicted results tended toward over-estimation. The results indicate that the model is a powerful tool for disinfestation applications, to predict the exposure time required to obtain lethal temperatures throughout grain kernel, so ensuring the total mortality of insects within it.

Keywords: Disinfestation; Fluidized bed; Hot air treatment; Mortality; Numerical method; Paddy

1. Introduction

For many decades, chemical methods have been used world-wide for controlling insect pests in agricultural products, such as fruits and cereal grains. However, because of increasing consumer dissatisfaction with the presence of residues in cereals and other foodstuffs, more interest has recently been directed towards thermal treatment methods. Heat disinfestation, conventional heating comprised of convective heat transfer from a medium, usually heated air or hot water, to the product surface, after which the heat flows inward from the surface to the center of the product, as well as combinations of convective and radiation heat transfer, have been extensively studied for controlling insect pests in fruits [1–11] and grains [12–22]. Technologies for the rapid high temperature disinfestation of grain have been available for many years; among these technologies is the fluidized bed which has interested many researchers [12–17] because of its great advantages in rapidly promoting heat transfer and thorough mixing, leading to uniform product properties. High temperature disinfestation of wheat in batch fluidized beds apparently performed very well, in completely killing all stages of insect pests when grain reached maximum temperature, up to 60–90 °C [12,13,15]. Evans et al. [16] carried out

* Corresponding author. Tel.: +66 (0) 2988 3666x241; fax: +66 (0) 2988 3655x241.
E-mail addresses: thanid@mut.ac.th, thanid_m@yahoo.com (T. Madhiyanon).

0017-9310/$ - see front matter © 2006 Elsevier Ltd. All rights reserved.
doi:10.1016/j.ijheatmasstransfer.2005.11.020

Nomenclature

A_t	surface area of a single cylindrical paddy kernel (m^2)
c	specific heat (J/kg K)
D_p	equivalent diameter of paddy (m)
h	heat transfer coefficient (W/m^2 K)
h_{fg}	latent heat (J/kg)
ΔH	heat of vaporization (J/kg)
J_0	Bessel function zero order
J_1	Bessel function first order
k	thermal conductivity of paddy (W/m K)
k_a	thermal conductivity of air (W/m K)
$2L$	length of paddy (m)
m_a	mass flow rate of air (kg/s)
m_w	moisture evaporated from a single paddy (kg water evaporated/one paddy)
m_p	mass of a single paddy (kg/one paddy)
m_b	total dry mass of paddy in the bed (kg)
m_{wp}	total mass of moisture evaporated in the bed (kg water evaporated)
M	moisture content (decimal dry basis)
Nu	Nusselt number (–)
Pr	Prandtl number (–)
r	radial distance from center of paddy (m)
Δr	space step in r-direction (m)
R	radius of paddy (m)
RC	fraction of recycled air (–)
S	Biot number of heat transfer (–)
t	time (s)
Δt	time step (s)
T	temperature (°C)
T_{abs}	absolute temperature (K)
$\overline{T_p}$	average temperature of paddy (°C)
T_{mean}	arithmetic mean temperature of air across the bed (°C)
v	velocity (m/s)
V_p	volume of a single paddy (m^3/one paddy)
W	air humidity ratio (kg water/kg dry air)
Δz	space step in z-direction (m)
z	axial distance from center of paddy (m)

Subscripts

a	air
amb	ambient
in	initial
i	inlet
i	space nodal grid index (radial axis)
j	space nodal grid index (axial axis)
mix	mixing condition of air
n	time nodal grid index
o	outlet
p	paddy
s	surface
v	vapor
w	water

Greek symbols

α	thermal diffusivity (m^2/s)
β_n	root of Bessel function (–)
ε	bed void (–)
ρ_a	density of air (kg/m^3)
ρ_b	bulk density of paddy (kg/m^3)
ρ_t	true density of paddy (kg/m^3)

experiments in a 0.5 ton per hour capacity continuous-flow fluidized bed, where grain was heated to at least 65 °C to obtain complete mortality of all immature stage of heat-tolerant species. The other rapid high temperature techniques for grain disinfestation are spouted bed, studied by Claflin and Evans [18] and Beckett and Morton [19], and pneumatic conveyor, studied by Sutherland et al. [20,21].

However, different insect species and stages, physical and thermal properties of products, and product size have different susceptibilities to heat treatment and furthermore, mortality is not related only to grain temperature; the rate at which the grain is heated is also important, and an increasing rate of heating by a higher medium temperature will create thermal shock and achieve significantly higher mortality [15,19,22]. Above tests for investigating conditions to meet insect mortality, therefore, are very labor-intensive and costly, and the results are only valid for the product tested under the specified conditions investigated. Furthermore, there is difficulty in measuring temperature distribution inside small products, such as cereals. Several researchers [9–12] have endeavored to develop mathematical methods to investigate the influences of the physical properties of fruit and heating methods on the evolution of temperature profiles inside fruits, and the heat transfer rate to the fruit core, which directly relates to insect mortality.

In an effort to predict maximum wheat temperature during the heat disinfestation process, Sutherland et al. [21] developed a model for wheat heat in a pneumatic conveyor, based only upon heat transfer mechanism, without including moisture transfer from the grain to the heated air. Thorpe [17] used his model to predict wheat temperature in a continuous-flow fluidized bed disinfestor. His model was derived from a simplified assumption of thermal equilibrium conditions between air leaving the bed and grain in the bed, which led to the model not necessarily dealing with the heat transfer coefficient. The model could not present the evolution of temperature profiles regarding the time required for complete mortality, which is useful for explaining insect death.

The purpose of the present study is to develop a model to investigate the influence of thermal treatments for paddy in a fluidized bed on dynamic changes in temperature profile and moisture content, as well as maximum paddy temperature obtained at a given exposure time. A model accounting only for heat transfer mechanism and another coupling both heat mass transfer phenomena are discussed in this study. The spherical and cylindrical coordinates for grain are compared in the simulation results from the heat diffusion equation, and the results obtained from analytical and numerical methods are also investigated for both coordinates. The validity of the model is checked with the experimental results. However, while the insect mortality test is not within the scope of this study, we anticipate that this research will provide valuable outcomes for further research into heat disinfestation for paddy by fluidized bed technique.

2. Transient thin-layer heat diffusion model

The thin-layer models for heat diffusion assume that grain diffusivity remains constant throughout the grain kernel, which is isotropic and in which shrinkage is negligible. The first model is based on one-dimensional heat diffusion for spherical geometry, as follows:

$$\frac{\partial T}{\partial t} = \alpha\left(\frac{\partial^2 T}{\partial r^2} + \frac{2}{r}\frac{\partial T}{\partial r}\right) \tag{1}$$

which is the equation of conservation of energy.

The initial and boundary conditions are:

Initial condition

$$t = 0, \quad 0 \leqslant r \leqslant R : T = T_{\text{in}} \tag{2}$$

Boundary condition

$$t > 0, \quad r = 0 : \frac{\partial T}{\partial r} = 0 \tag{3}$$

$$r = R : k\frac{\partial T}{\partial r} = h(T_{\text{a}} - T_{\text{s}}) \tag{4}$$

The convection boundary equation (Eq. (4)) does not account for moisture loss from the kernel surface during the heat disinfestation process. The average grain temperature $\overline{T_{\text{P}}}(t)$ is obtained by integrating $T(r,t)$ over the sphere volume.

$$\overline{T_{\text{P}}}(t) = \frac{4\pi}{V_{\text{P}}}\int_0^R r^2 T(r,t)\,\mathrm{d}r \tag{5}$$

The second model is based on cylindrical coordinates with similar assumptions to the first model, and may be expressed as follows:

$$\frac{\partial T}{\partial t} = \alpha\left(\frac{\partial^2 T}{\partial r^2} + \frac{1}{r}\frac{\partial T}{\partial r} + \frac{\partial^2 T}{\partial z^2}\right) \tag{6}$$

which is the cylindrical geometry of the grain kernel, as shown in Fig. 1. The initial and boundary conditions are described as follows:

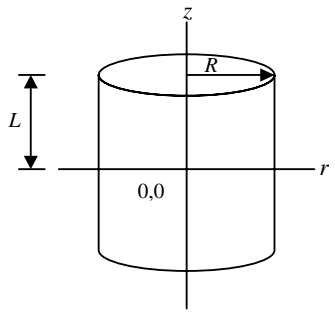

Fig. 1. The cylindrical geometry of grain kernel used for simulation.

Initial conditions

$$t = 0, \quad 0 \leqslant r \leqslant R : T = T_{\text{in}} \tag{7}$$

$$0 \leqslant z \leqslant L : T = T_{\text{in}} \tag{8}$$

Boundary conditions

$$t > 0, \quad r = 0, \ 0 \leqslant z \leqslant L : \frac{\partial T}{\partial r} = 0 \tag{9}$$

$$z = 0, \ 0 \leqslant r \leqslant R : \frac{\partial T}{\partial z} = 0 \tag{10}$$

$$r = R, \ 0 \leqslant z \leqslant L : k\frac{\partial T}{\partial r} = h(T_{\text{a}} - T_{\text{s}}) \tag{11}$$

$$z = L, \ 0 \leqslant r \leqslant R : k\frac{\partial T}{\partial z} = h(T_{\text{a}} - T_{\text{s}}) \tag{12}$$

The average temperature of grain in a cylindrical shape is defined by:

$$\overline{T_{\text{P}}}(t) = \frac{2\pi}{V_{\text{P}}}\int_0^L \int_0^R rT(r,t)\,\mathrm{d}r\,\mathrm{d}z \tag{13}$$

For a sphere with an aid of analogy between heat and mass diffusion problem, the solution form of mass diffusion in a sphere proposed by Vernaud [23] is used, as the solution to Eqs. (1)–(4), in which the solution is in the form containing temperature rather than the concentration of diffusing substance as a space-time dependent variable, and may be expressed as

$$\frac{T - T(r,t)}{T - T_{\text{in}}} = \frac{2SR}{r}\sum_{n=1}^{\infty}\frac{1}{\left(\beta_n^2 + S^2 - S\right)}\frac{\left(\sin\frac{\beta_n r}{R}\right)}{\sin\beta_n}\exp\left[-\frac{\beta_n^2}{R^2}\alpha t\right] \tag{14}$$

where the β_ns are roots of the following equation:

$$\beta_n\cot\beta_n + S - 1 = 0 \tag{15}$$

and the dimensionless number S is a Biot number for heat transfer, which is an indication of internal thermal resistance to external boundary layer thermal resistance, and may be expressed as

$$S = \frac{hR}{k} \tag{16}$$

For a cylinder, the solution of a two-dimensional, time-dependent heat conduction problem is equivalent to the

product of the solution of two one-dimensional transient heat conduction problems [24], thus the solution to determine the temperature profile of a finite cylinder associating to Eqs. (6)–(12) is

$$\frac{T-T(r,z,t)}{T-T_{\text{in}}}=\left[\frac{T-T(r,t)}{T-T_{\text{in}}}\right]_{\text{infinite cylinder}}\times\left[\frac{T-T(z,t)}{T-T_{\text{in}}}\right]_{\text{infinite plate}} \tag{17}$$

where the solutions for infinite cylinder and infinite plate are again adapted from the solution of Vernaud [23], as follows:

For infinite cylinder (non-steady state with finite rate of convection heat transfer)

$$\left[\frac{T-T(r,t)}{T-T_{\text{in}}}\right]_{\text{infinite cylinder}}=\sum_{n=1}^{\infty}\frac{2SJ_0\left(\beta_n\frac{r}{R}\right)}{\left(\beta_n^2+S^2\right)J_0\beta_n}\exp\left[-\frac{\beta_n^2}{R^2}\alpha t\right] \tag{18}$$

where β_ns are roots of

$$\beta_n J_1(\beta_n)-SJ_0(\beta_n)=0 \tag{19}$$

which J_0 and J_1 are Bessel function zero and first order, respectively, and may be described as [25]

$$J_0(\beta_n)=1-\frac{\beta_n^2}{2^2}+\frac{\beta_n^4}{2^2\cdot 4^2}-\frac{\beta_n^6}{2^2\cdot 4^2\cdot 6^2}+\dots \tag{20}$$

$$J_1(\beta_n)=\frac{\beta_n}{2}-\frac{\beta_n^3}{2^2\cdot 4}+\frac{\beta_n^5}{2^2\cdot 4^2\cdot 6}-\frac{\beta_n^7}{2^2\cdot 4^2\cdot 6^2\cdot 8}+\dots \tag{21}$$

where β_n can be simultaneously solved from Eqs. (19)–(21) by iteration procedure.

For infinite plate (non-steady state with finite rate of convection heat transfer)

$$\left[\frac{T-T(z,t)}{T-T_{\text{in}}}\right]_{\text{infinite plate}}=\sum_{n=1}^{\infty}\frac{2S\cos\left(\beta_n\frac{z}{L}\right)}{\left(\beta_n^2+S^2+S\right)\cos\beta_n}\times\exp\left[-\frac{\beta_n^2}{L^2}\alpha t\right] \tag{22}$$

where L is half plate thickness, β_ns are positive roots of

$$\beta_n\tan\beta_n=S \tag{23}$$

Numerical solutions were also used to solve the partial differential equations with mixed boundary conditions, and the corresponding results were compared with the computed results obtained from analytical solutions (Eqs. (14) and (17)). The finite-difference approach was used to discretize the derivative in partial differential equations into a system of algebraic equations, the well-known Crank–Nicholson implicit method was chosen to solve spherical coordinate problems and an explicit method for cylindrical coordinate problems. To simulate a heat diffusion thin-layer model, it is reasonably assumed that air temperature remains unchanged when passing through a thin layer of grain; thus, the thermodynamic properties of air used for calculation can be evaluated at the inlet air temperature.

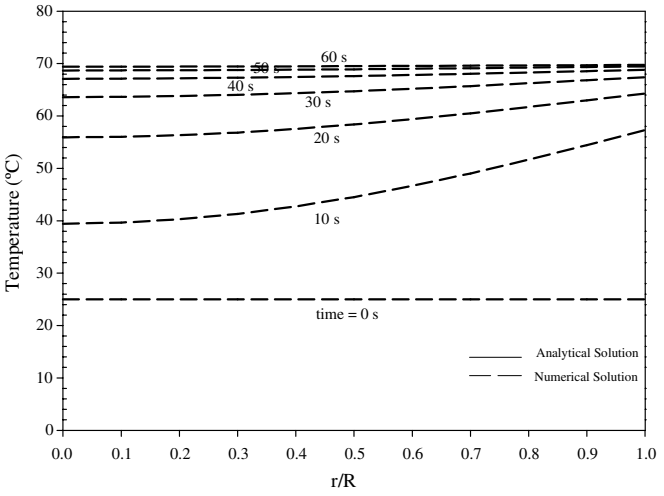

Fig. 2. Comparison of temperature profiles inside a spherical paddy kernel between obtaining from numerical and analytical solution of thin layer model.

The heat transfer coefficient correlation and the thermal properties of paddy can be found in the relevant section of this study. The moisture content of the paddy was assumed to be constant at 14% dry throughout the heating period, which is generally in the range for the moisture content of stored paddy.

Fig. 2 shows the computed temperature distribution inside a spherical paddy kernel with 3.5 mm equivalent diameter at inlet air temperature of 70 °C and air velocity of 2.5 m/s. The temperature data of both solutions, obtained from analytical and numerical methods, appeared to be indistinguishable. The intra-temperatures became uniform across the grain kernel and were elevated to inlet air temperature within 60 s of commencement.

Figs. 3 and 4 show predicted temperature profiles inside a paddy kernel assumed to be cylindrical in the air condi-

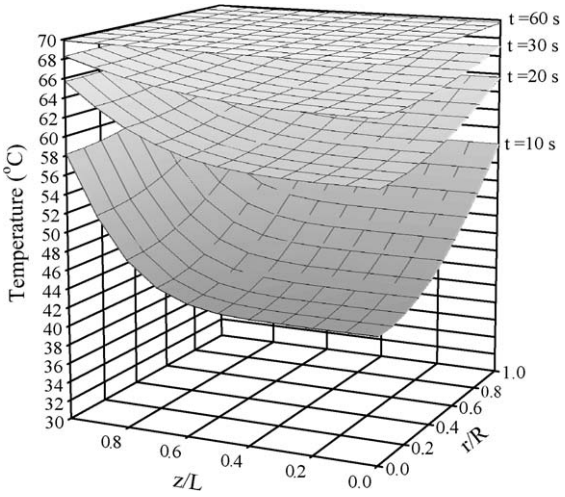

Fig. 3. Temperature profiles inside a cylindrical paddy kernel computed by analytical solution at inlet air temperature of 70 °C.

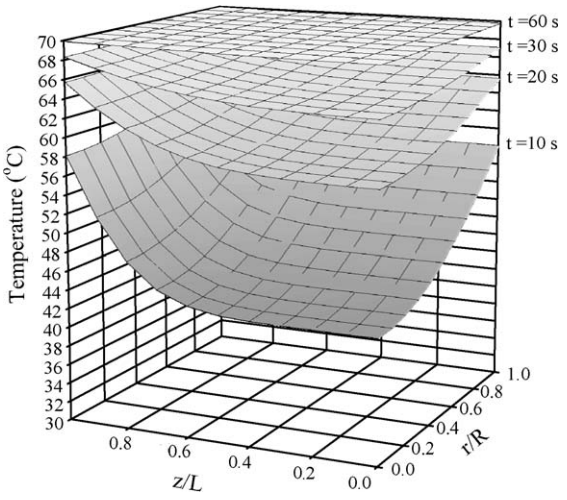

Fig. 4. Temperature profiles inside a cylindrical paddy kernel computed by numerical solution at inlet air temperature of 70 °C.

tions for an assumed spherical paddy kernel. A cylindrical paddy kernel has a diameter of 2.5 mm and length of 9.5 mm. In Fig. 3, the temperature profiles determined by analytical solution are identical with those determined by numerical solution, as shown in Fig. 4. It is clearly seen that temperature along with the radius became uniform more rapidly than along with the length, however, there is no evidence of temperature gradient within a kernel, either in the radial or axial direction, exiting after 60 s of heating. This is consistent with the computed results for a spherical paddy kernel.

Fig. 5 presents the average grain temperature of a spherical grain kernel compared with that of the cylindrical grain kernel. It is evident that there is almost no difference in the average grain temperature between both coordinates.

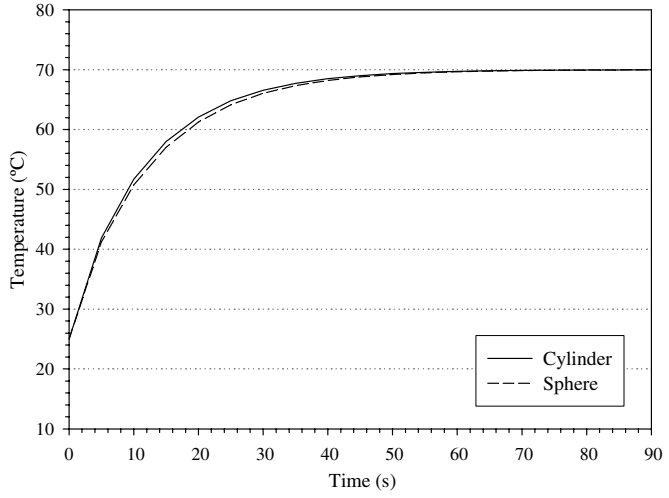

Fig. 5. Comparison between predicted average paddy temperature of a spherical and cylindrical shape at inlet air temperature of 70 °C.

3. Model development for heat disinfestation in a fluidized bed

Even though the thin-layer heat diffusion models discussed above can provide temperature profiles inside grain kernels, which is necessary for analyzing the mortality of all insects inside grain kernels, they alone cannot sufficiently describe the transport process phenomena in deep bed grain disinfestations, such as fluidized bed disinfestation. They must be incorporated into a deep bed simulation model derived from mass and energy conservation laws. Because there are differences in heat diffusion rates between axial and radial directions, a paddy kernel was assumed to be a cylindrical object, as discussed in Section 2, and a geometric cylinder should be more appropriate than a spherical shape for paddy. Thus, cylindrical coordinates of heat diffusion equation were used in the simulation.

The following assumptions were made in developing the model:

1. Paddy kernels are uniform in size and internally homogeneous.
2. In the first fluidized bed disinfestation model, assuming that any change in the moisture content of stored grain is very small and has no effect on the process, moisture loss from the grain surface was not accounted for. However, in the second model, moisture loss and the corresponding heat of evaporation were added to the convective boundary conditions and energy equation, respectively.
3. The effects of heat conduction and moisture transfer between the grains, and heat loss, were not accounted for.
4. The accumulation of thermal energy and water vapor in the air in the bed was disregarded.
5. It was assumed that the grains were well mixed and had the same temperature and moisture content at any location in the bed.
6. With respect to up-modulating high air temperature and high air flow rate, as in a fluidized bed application, it was assumed the exit air and the grains in the bed had not reached a condition of thermal equilibrium.

To simulate heat disinfestation in a fluidized bed system, in which part of the exhaust air is recycled for energy-saving reasons, the system is divided into a series of elementary control volumes, as shown in Fig. 6. The basic principles of the laws of mass and energy conservation, accounting for convective heat transfer and mass transfer based on the empirical model fitted from the experimental data, are employed to each elementary control volume, leading to a set of governing equations, as follows:

3.1. Fluidized-bed chamber (cv. 1)

The appreciable fluidization of grains accounting for a current model is characterized by assuming the well-mixed

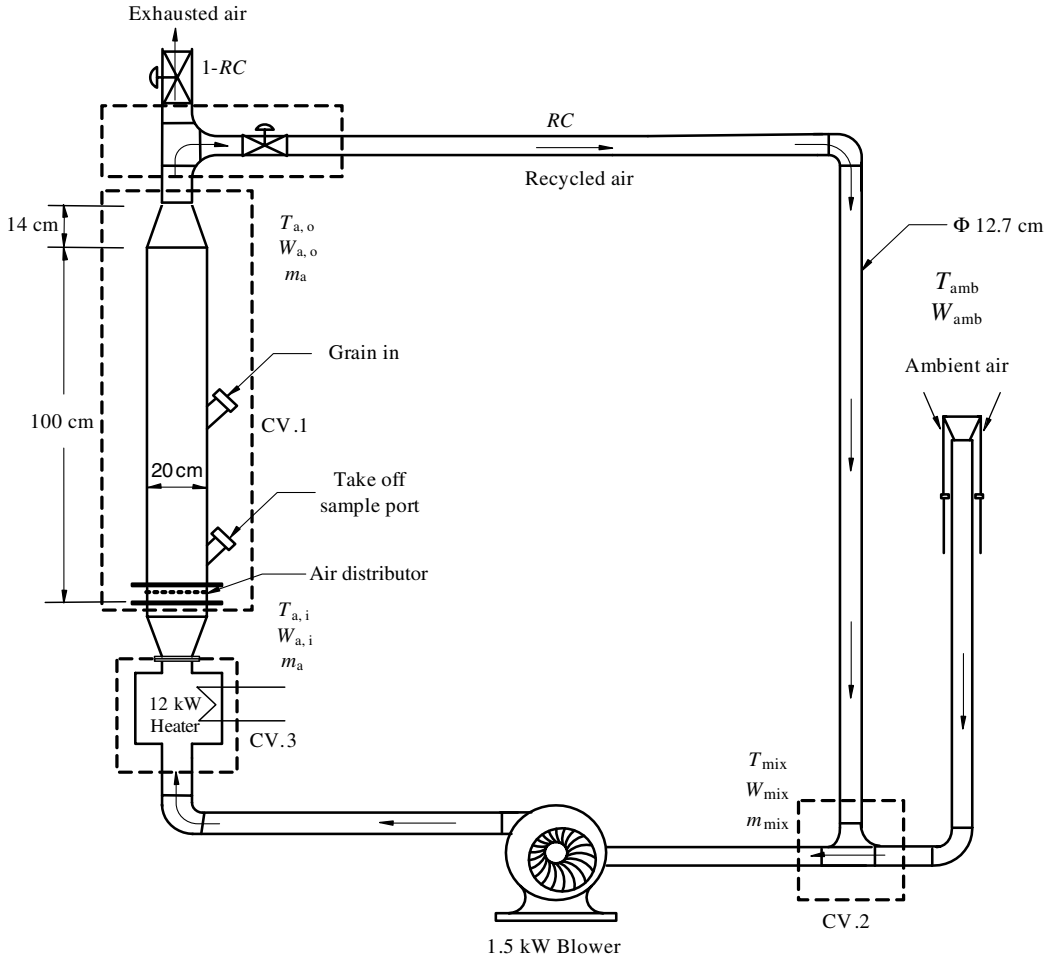

Fig. 6. Schematic diagram of batch fluidized bed disinfestor.

condition of grains (Assumption 5) so as all grains elsewhere inside the bed are in the same moisture content and temperature.

3.1.1. Macroscopic mass balance

Control volume 1 (cv. 1), as shown in Fig. 6, represents the fluidized-bed chamber. By employing Assumption 4, that the accumulation rate of water vapor in the air within the bed is not accounted for, the physical meaning of the law of mass conservation may be written as

[Mass of moisture evaporated from grain]

= [Change in moisture of grain]

= [Change in humidity of air]

which are mathematically expressed as follows:

$$m_{wb} = m_b \frac{dM}{dt} \tag{24}$$

and

$$-m_b \frac{dM}{dt} = m_a(W_{a,o} - W_{a,i}) \tag{25}$$

term $\left[\frac{dM}{dt}\right]$ can be determined by applying Eq. (31) and is not implied if moisture loss is not accounted for.

3.1.2. Macroscopic energy balance

With the Assumption 4 that the accumulation of thermal energy in the air in the bed is negligible. The exchange energy between the air across the bed and the grains gives a relationship, as follows:

[Enthalpy change of air across bed]

= [Internal change of the grain in the bed]

+ [Energy used for evaporation of moisture evaporated from the grain]

+ [Energy for increasing the temperature of the moisture evaporated to the temperature of the air]

The last term on the right-hand side of the above equation may be omitted when compared with other terms, and is mathematically expressed as

$$m_a c_a(T_{a,i} - T_{a,o}) + m_a c_v(W_{a,i}T_{a,i} - W_{a,o}T_{a,o}) = m_b(c_p + c_w M_{in})\frac{d\overline{T_p}}{dt} + m_{wb}\Delta H \tag{26}$$

which is a non-equilibrium thermal condition. The last term on the right hand side of Eq. (26) ($m_{wb}\Delta H$) is respon-

sible for the heat of evaporation and is not considered when the moisture evaporated is negligible.

3.1.3. Heat and mass transfer of a single grain

Heat transfer of a single grain is governed by a heat diffusion equation for cylindrical geometry, with appropriate initial and boundary conditions, as described by Eqs. (6)–(12). In the second fluidized bed heat disinfestation model, including accounting for moisture loss from the grain surface, boundary equations (11) and (12) are replaced by the following equations:

$$t > 0, \quad r = R, \ 0 \leqslant z \leqslant L : k\frac{\partial T}{\partial r} = h(T_a - T_s) - m_w\frac{\Delta H}{A_t} \tag{27}$$

$$z = L, \ 0 \leqslant r \leqslant R : k\frac{\partial T}{\partial z} = h(T_a - T_s) - m_w\frac{\Delta H}{A_t} \tag{28}$$

moisture loss of a single grain (m_w) can be determined from

$$m_w = m_p\frac{dM}{dt} \tag{29}$$

where

$$m_p = \rho_t V_p \tag{30}$$

Term $\left[\frac{dM}{dt}\right]$ is the rate of change in moisture content in which the relationship between the moisture content (M) and the disinfestation time (t) was evaluated by fitting corresponding data from the present experiments carried out under the various heating temperatures. A exponential form correlation performed by least square method was found to provide good agreement between the experimental data and the correlation, and can be expressed as

$$M(t) = M_{in} - \exp(a)\exp(b\ln T_{a,i})\exp(c\ln t) \tag{31}$$

where t is disinfestation time (s), and a, b, c are constant parameters for the various disinfestation temperatures, shown below:

Air temperature (<75 °C): $a = -20.3969, b = 4.3215, c = 0.4883$.
Air temperature (<110 °C): $a = -9.7093, b = 1.8136, c = 0.5778$.
Air temperature (<150 °C): $a = -6.7201, b = 1.2184, c = 0.4234$.

3.2. Mixing section (cv. 2)

Because the system employs exhaust air recycling, the ambient air temperature must be elevated to inlet air temperature and hence the mixing temperature must be determined before assessing the energy required to heat the mixed air to desirable inlet air temperature. Using the basic knowledge of energy conservation, the mixing temperature can be determined by the following equation:

$$m_{mix}c_aT_{mix} + m_{mix}W_{mix}(h_{fg} + c_vT_{mix}) - (1 - RC)m_ac_aT_{amb} - (1 - RC)m_aW_{amb}(h_{fg} + c_vT_{amb}) - RCm_ac_aT_{a,o} - RCm_aW_{a,o}(h_{fg} + c_vT_{a,o}) = 0 \tag{32}$$

The mass balance for the air phase is written as

$$m_{mix} = m_a \tag{33}$$

and the mass balance for the vapor phase is expressed as

$$W_{mix} = RCW_{a,o} + (1 - RC)W_{amb} \tag{34}$$

The increase in the humidity of the air leaving the bed, by moisture transferred from the surface of stored grains, which usually have a relatively low moisture content and for which it is difficult to shed moisture, is very small and can be approximately unchanged when the air leaves the bed. Thus Eqs. (25) and (34) can be simplified to

$$W_{a,o} \cong W_{a,i} \tag{35}$$

and

$$W_{mix} \cong W_{a,o} \tag{36}$$

3.3. Heating chamber (cv. 3)

The energy input to heat air before entering the fluidized-bed chamber can be calculated from

$$Q = m_{mix}(c_a + W_{mix}c_v)(T_{a,i} - T_{mix}) \tag{37}$$

3.4. Properties and thermodynamic equations

The correlation of heat transfer subjected to the fluidized bed reported by Kunii and Levenspiel [26] was selected for simulation, and may be expressed as

$$Nu = 2 + 0.6Re^{0.5}Pr^{0.33} \tag{38}$$

where $h = Nuk_a/D_p$, $Re = \rho_a v_a D_p/\mu_a$; $(0.1 < Re < 10^4)$ and $Pr = c_a\mu_a/k_a$.

In which D_p equates with the diameter of a grain. Although Eq. (38) is primary correlated for spherical particles in the fluidized bed but it is permitted for non-spherical particle as well.

Expressions for properties of product and thermodynamics equations for air–water systems (Eqs. (49)–(60)) are listed in Tables 1 and 2. Eqs. (52)–(54) are used to calculate true density of paddy ρ_t and hence the mass of one grain may be determined from Eq. (30).

4. Solution algorithm

The solution procedure for the governing equation involves the following steps:

1. Parameters, i.e. inlet air temperature ($T_{a,i}$), inlet air humidity ($W_{a,i}$), which is approximately equal to ambient air humidity (W_{amb}), initial moisture content (M_{in}), initial grain temperature, air mass flow rate (m_a), dry

Table 1
Properties of paddy used for simulation [27–29]

Equations	Property	Expression	References	Units
(49)	ΔH	$\Delta H = (2502 - 2.386\overline{T}_p)(1 + 2.496\exp(-21.733M)) \times 10^3$	[27]	J/kg H_2O
(50)	c_p	$c_p = 1.11 \times 10^3 + 44.8(M/(1+M))$	[27]	J/kg
(51)	k	$k = 0.0863 + 0.00134(M/(1+M))$	[28]	W/m K
(52)	ε	$\varepsilon = 0.62 - 0.25(M/(1+M))$	[29]	Decimal
(53)	ε	$\varepsilon = 1 - \rho_b/\rho_t$	[30]	Decimal
(54)	ρ_b	$\rho_b = 552 + 282(M/(1+M))$	[29]	kg/m^3

Table 2
Thermodynamics of air and water system [27,30]

Equations	Property	Expression	Units
(55)	c_a	$c_a = 1.00926 \times 10^3 - 4.0403 \times 10^{-2}T + 6.1759 \times 10^{-4}T^2 - 4.097 \times 10^{-7}T^3$	J/kg K
(56)	k_a	$k_a = 2.425 \times 10^{-2} + 7.889 \times 10^{-5}T - 1.790 \times 10^{-8}T^2 - 8.570 \times 10^{-12}T^3$	W/m K
(57)	ρ_a	$\rho_a = 101.325/(0.287T_{abs})$	kg/m^3
(58)	μ_a	$\mu_a = 1.691 \times 10^{-5} + 4.984 \times 10^{-8}T - 3.187 \times 10^{-11}T^2 + 1.319 \times 10^{-14}T^3$	kg/m s
(59)	c_v	$c_v = 1.883 \times 10^3 - 1.6737 \times 10^{-1}T + 8.4386 \times 10^{-4}T^2 - 2.6966 \times 10^{-7}T^3$	J/kg K
(60)	c_w	$c_w = 2.8223 \times 10^3 + 11.828T - 3.5043 \times 10^{-2}T^2 + 3.601 \times 10^{-5}T^3$	J/kg K

mass of paddy in bed (m_b), air recycling ratio (RC), and superficial air velocity, are taken as input parameters to initiate the simulation.

2. For each given time step, by applying the heat diffusion equation for cylindrical coordinates (Eq. (6)) and appropriate initial and boundary conditions (Eqs. (7)–(12)) or replacing Eqs. (11) and (12) with Eqs. (27) and (28) where accounting for moisture loss, temperature profiles inside the kernel, in respect to a given time step, can be determined. Moisture loss from one grain (m_w) appeared in the convection boundary conditions (Eqs. (27) and (28)) can be evaluated from Eqs. (29)–(31). The temperature of the air decreases as it flows throughout the bed; thus, to calculate the corresponding heat transfer coefficient, the properties of the air are evaluated at an average temperature between inlet and exit air. However, the exit temperature ($T_{a,o}$) is not yet known; therefore, in this step, an iterative solution is necessary and $T_{a,o}$ is assumed as initial estimate to determine the heat transfer coefficient and the solution of the heat diffusion equation, respectively. The implicit finite difference with the discrete grid of the cylindrical object, as shown in Fig. 7, was advanced. The finite difference representing the governing equations, including accounting for moisture loss, may be written in the following form:

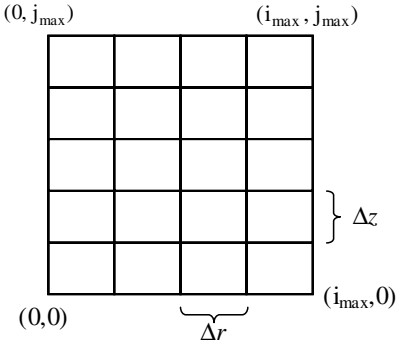

Fig. 7. Numerical grids for a one-forth cylindrical object for the governing equations.

Case 1: $i = 0, j = 0$

$$T_{0,0}^{n+1} = (1 - 4F_r - 2F_z)T_{0,0}^n + 4F_rT_{1,0}^n + 2F_zT_{0,1}^n \tag{39}$$

Case 2: $i = 0, j = j_{max}$

$$T_{0,j_{max}}^{n+1} = (1 - 4F_r - 2F_z\beta_N)T_{0,j_{max}}^n + 2F_zT_{0,j_{max}-1}^n + 4F_rT_{1,j_{max}}^n + 2F_z\gamma_N - 2F_z\left(\frac{\Delta z}{k}\right)\left(\frac{m_w\Delta H}{A_t}\right) \tag{40}$$

Case 3: $i = i_{max}, j = 0$

$$T_{i_{max},0}^{n+1} = (1 - 2F_r\beta_M - 2F_z)T_{i_{max},0}^n + 2F_r\gamma_M + 2F_rT_{i_{max}-1,0}^n + 2F_zT_{i_{max},1}^n - \left(1 + \frac{1}{2i}\right)\left(\frac{2F_r\Delta r}{k}\right)\left(\frac{m_w\Delta H}{A_t}\right) \tag{41}$$

Case 4: $i = i_{max}, j = j_{max}$

$$T_{i_{max},j_{max}}^{n+1} = (1 - 2F_r\beta_M - 2F_z\beta_N)T_{i_{max},j_{max}}^n + 2F_r\gamma_M + 2F_z\gamma_N + 2F_rT_{i_{max}-1,j_{max}}^n + 2F_zT_{i_{max},j_{max}-1}^n - 2\left(\frac{F_z\Delta z}{k}\right)\left(\frac{m_w\Delta H}{A_t}\right) - \left(1 + \frac{1}{2i}\right)\left(\frac{2F_r\Delta r}{k}\right)\left(\frac{m_w\Delta H}{A_t}\right) \tag{42}$$

Case 5: $i = i_{\max}, j = 1,2,3,\ldots,j_{\max}-1$

$$T^{n+1}_{i_{\max},j} = (1-2F_r\beta_M - 2F_z)T^n_{i_{\max},j} + 2F_r\gamma_M + 2F_{\mathrm{r}}T^n_{i_{\max}-1,j} + F_zT^n_{i_{\max},j+1} + F_{\mathrm{z}}T^n_{i_{\max},j-1} - \left(1+\frac{1}{2i}\right)\left(\frac{2F_{\mathrm{r}}\Delta r}{k}\right)\left(\frac{m_{\mathrm{w}}\Delta H}{A_{\mathrm{t}}}\right) \quad (43)$$

Case 6: $i = 1,2,3,\ldots,i_{\max}-1, j = j_{\max}$

$$T^{n+1}_{i,j_{\max}} = (1-2F_r - 2F_z\beta_{\mathrm{N}})T^n_{i,j_{\max}} + \left(1+\frac{1}{2i}\right)F_{\mathrm{r}}T^n_{i+1,j_{\max}} + 2F_z\gamma_N + \left(1-\frac{1}{2i}\right)F_{\mathbf{r}}T^n_{i-1,j_{\max}} + 2F_zT^n_{i,j_{\max}-1} - \left(\frac{2F_z\Delta z}{k}\right)\left(\frac{m_{\mathrm{w}}\Delta H}{A_{\mathrm{t}}}\right) \quad (44)$$

Case 7: $i = 1,2,3,\ldots,i_{\max}-1, j = 0$

$$T^{n+1}_{i,0} = (1-2F_r-2F_z)T^n_{i,0} + \left(1+\frac{1}{2i}\right)F_rT^n_{i+1,0} + \left(1-\frac{1}{2i}\right)F_rT^n_{i-1,0} + 2F_zT^n_{i,1} \quad (45)$$

Case 8: $i = 0, j = 1,2,3,\ldots,j_{\max}-1$

$$T^{n+1}_{0,j} = (1-4F_r-2F_z)T^n_{0,j} + 4F_rT^n_{1,j} + F_zT^n_{0,j+1} + F_zT^n_{0,j-1} \quad (46)$$

Case 9: $i = 1,2,3,\ldots,i_{\max}-1, j = 1,2,3,\ldots j_{\max}-1$

$$T^{n+1}_{i,j} = (1-2F_r-2F_z)T^n_{i,j} + \left(1+\frac{1}{2i}\right)F_rT^n_{i+1,j} + \left(1-\frac{1}{2i}\right)F_rT^n_{i-1,j} + F_zT^n_{i,j+1} + F_zT^n_{i,j-1} \quad (47)$$

The stability criterions for the above equations are

$$F_r + F_z \leqslant \frac{1}{2} \quad (48)$$

where

$$F_r = \frac{\alpha\Delta t}{\Delta r^2}; \quad \alpha = \frac{k}{\rho_{\mathrm{t}}c_{\mathrm{p}}}$$

$$F_z = \frac{\alpha\Delta t}{\Delta z^2}$$

$$\beta_N = 1 + \left(\Delta z\frac{h}{k_{\mathrm{a}}}\right)$$

$$\beta_M = 1 + \left(\left(1+\frac{1}{2i}\right)\Delta r\frac{h}{k_{\mathrm{a}}}\right)$$

$$\gamma_M = \left(1+\left(\frac{1}{2i}\right)\right)\left(\Delta r\frac{h}{k_{\mathrm{a}}}\right)T_{\mathrm{mean}}; \quad T_{\mathrm{mean}} = \frac{T_{\mathrm{a,i}}+T_{\mathrm{a,o}}}{2}$$

$$\gamma_N = \left(\Delta z\frac{h}{k_{\mathrm{a}}}\right)T_{\mathrm{mean}}$$

In the above equations, terms involving evaporated moisture are neglected if not considering moisture loss during the heat disinfestation process.

3. Knowing the temperature accompanied by each node inside the grain kernel, the average temperature can be resolved by applying Simpson's method to Eq. (13).
4. From the mass and energy conservation equations (Eqs. (24)–(26)), the exit air temperature is determined and compared to the initial estimated value. If the difference in result is not within an acceptable level, the initial estimate will be changed to the update result, and the entire procedure repeated until the difference in the exit air temperature is less than 0.005 °C, which is considered insignificant based on practical considerations. Once the solution regarding the fluidized-bed chamber section has been assembled, the simulation will be continued further for subsequent sections, by solving Eq. (25) to determine the change in humidity ratio of the air leaving the bed, Eqs. (32) and (34) to calculate mixing temperature and mixing humidity ratio of the air departing from mixing section and Eq. (37) to find out heat input. In the specific event of not accounting moisture evaporated, Eqs. (25) and (34) are omitted and consequently replaced by Eqs. (35) and (36).
5. The final conditions of the air throughout the bed and the grain within the bed, accomplished by the procedure in steps 1–4, are now initialized for the condition of the next time step. The entire procedure is repeated until the end of the disinfestation period.

5. Experiments

Experiments were conducted to validate the simulation results of changes in air and grain temperatures during the heat treatment process.

5.1. Materials

Experiments with paddy heating were conducted using a fluidized bed batch disinfestor, as shown in Fig. 6. The fluidized-bed chamber was made of stainless steel and was of a cylindrical shape, 20 cm in diameter and 140 cm in height. The chamber and connected air ducts were insulated with fiberglass insulation 25 mm in thickness. Hot air was distributed to the bottom of the chamber through an air distributor plate. Air was heated by electric heaters with a total capacity of 12 kW. The inlet air temperatures were automatically controlled by PDI temperature controller, with an accuracy of ±1 °C. Temperatures were measured by a data logger and a temperature indicator with an accuracy of ±1 °C connected to a type K thermocouple. Air velocity was measured by hot wire anemometer with an accuracy of ±5%. A mechanical variable speed drive was used to regulate blower motor speed to attain the desired airflow rate.

5.2. Experimental set-up and conditions

Dried long-grain rough rice (paddy) with moisture contents in the range 12–14% (dry basis) was selected as the

test material. 0.8 kg of paddy, which created a non-fluidized bed height of 4 cm, was loaded into the fluidized chamber for each experiment. To guarantee complete fluidization of paddy is attained, the fluidization velocity of 2.5 m/s, which is equal to 1.5 times of the calculated minimum fluidization velocity (1.65 m/s), was used and held constant, and the percentage-air-recycled ratio was set at 20% for each experiment. The exit air temperatures were measured at a distance of 85 cm above the air distributor. The paddy samples were taken for determination of temperature and moisture content at intervals of 10 s. To ensure that the process mechanism was not deviated from, or disturbed by collecting the samples, the process with same desired conditions was restarted after collecting each sample until the target time was reached. The inlet air temperatures were set at 60, 80, 100 and 120 °C, respectively.

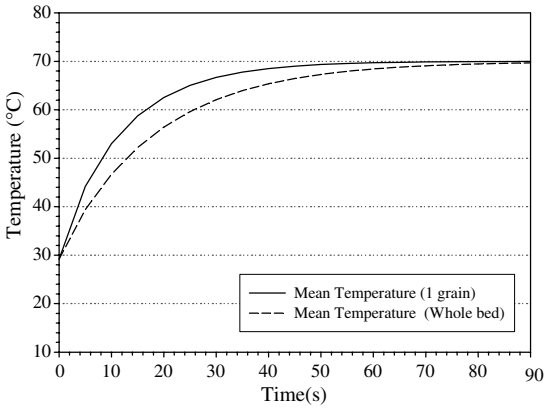

Fig. 9. Comparison of simulated average paddy temperature between computational from thin layer and fluidized bed models at inlet air temperature of 70 °C.

6. Result and discussion

6.1. Prediction of temperature gradient inside individual paddy kernel

Fig. 8 presents the moisture profile inside individual paddy kernels at an air temperature of 70 °C computed by the fluidized bed model, in which the moisture evaporation effect was not accounted for. Heat flow patterns similar to the thin-layer model (Fig. 4) were observed, but different times were required for temperature equalization. The temperature throughout the grain kernel, as predicted by the fluidized bed model, attained uniformity more slowly than that predicted by the thin-layer model. This is because the air temperature used for calculating heat transfer coefficient and heat transfer rate in the thin layer model was assumed unchanged and was equal to the inlet air temperature, whilst the fluidized bed model acknowledges the effects of air temperature changes within the bed. Therefore, the arithmetic mean of the air temperatures across the bed was used in calculation.

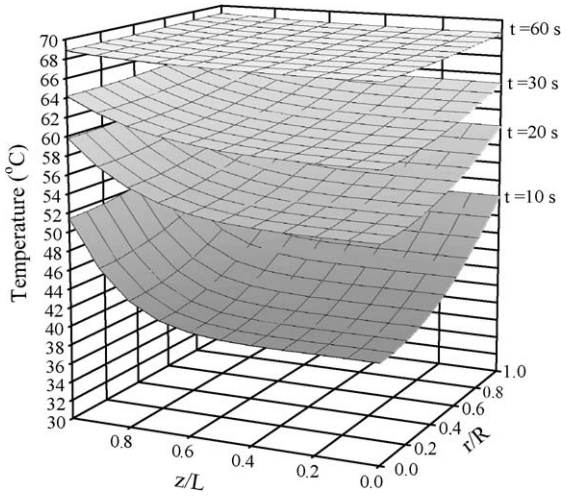

Fig. 8. Temperature profiles inside a cylindrical paddy kernel computed by fluidized bed model excluding moisture loss effect at inlet air temperature of 70 °C.

To provide a clearer picture, the average temperatures of grain for both the thin layer and fluidized bed models, corresponding to temperature distribution data in Figs. 4 and 8 were plotted, as shown in Fig. 9. It is indicative of more rapid changes in grain temperature in the thin layer model, leading to incorrect determination of the lethal time required for mortality of insects inside grain kernels.

6.2. Experimental validation without accounting for moisture loss

Fig. 10(a–c) shows the experimental and predicted average grain temperatures and exit air temperatures at inlet air temperatures of 60, 80, 100 and 120 °C, respectively. The model excluding moisture loss effect over-predicted experimental results where the dynamic changes in predicted values progressed more quickly than in the experimental values and resulted in predicting grain and exit air temperatures approaching inlet air temperature at the end period, whilst that did not happen in the experiments. It was also noticeable that use of a higher inlet air temperature resulted in higher discrepancies between experimental and simulation results. Over-prediction of grain and exit air temperatures was assumed to be caused by neglecting evaporation heat for moisture reduction during heat treatment, leading to over-accelerating the changes in the predicted air and grain temperatures. In an attempt to investigate the relationship between moisture reduction and changes in grain and air temperatures, the moisture content of grain versus time under several inlet air temperatures were plotted, together with air and grain temperatures, as shown in Fig. 10. It is clearly illustrated that the moisture content of the grain decreases with heating time, especially at high inlet air temperatures, and this could affect the predictiveness of the model.

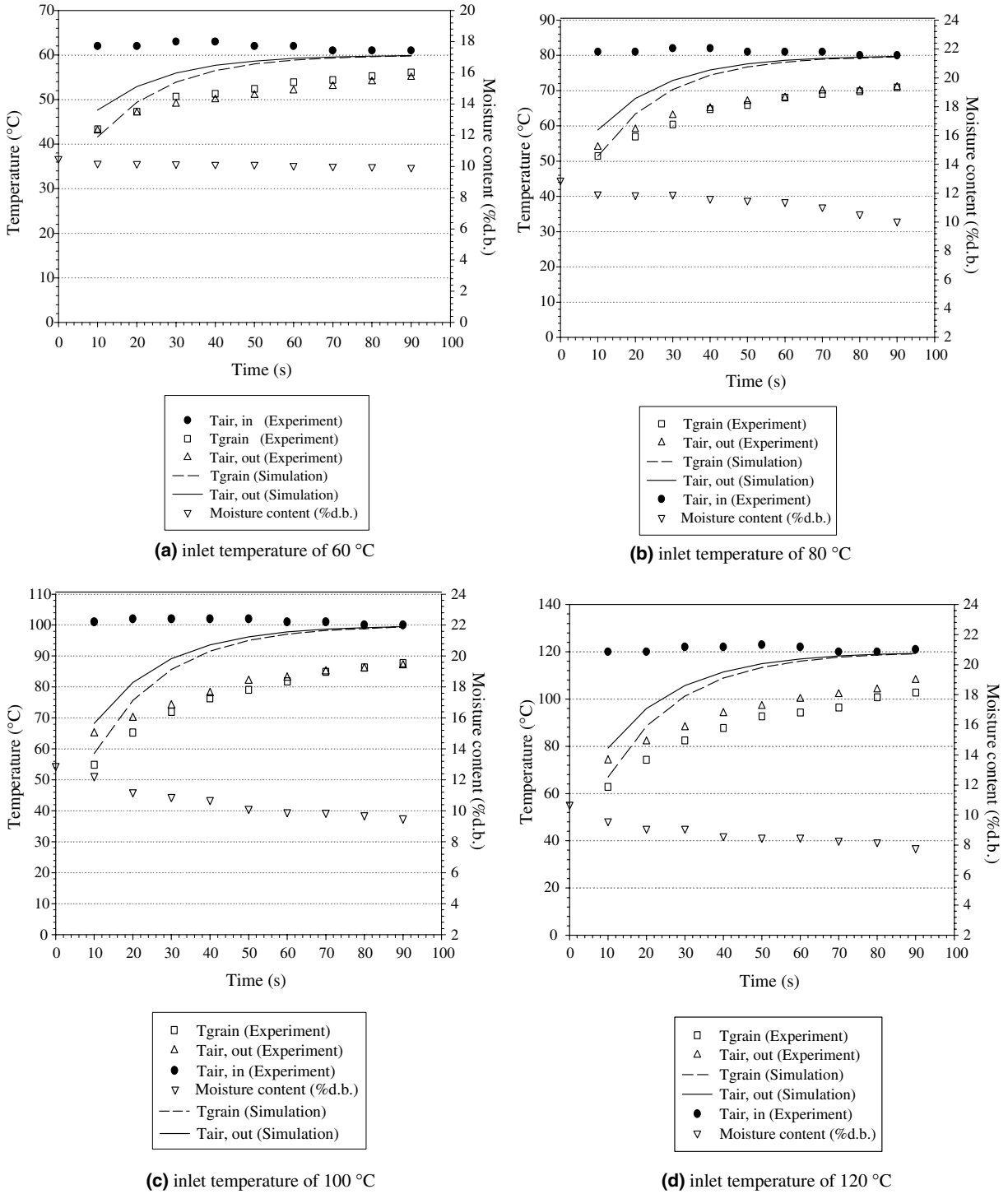

Fig. 10. Simulation and experimental results of heat disinfestation fluidized bed model excluding moisture transfer effect.

6.3. Simulation of coupled heat and mass transfer in fluidized bed disinfestor

The previous section indicated that a model in which the influence of moisture evaporation on energy exchange between air and grain was excluded did not provide a realistic prediction. Fig. 10 indicates that only 1.0% d.b. of average moisture reduction may significantly affect the predicted results. To improve the model predicting grain and exit air temperatures, moisture losses and the relative energy used for evaporation are taken into account, and then the solution is resolved by simultaneously combining the heat exchange contribution and the moisture transfer in the bed. The experimental data in Fig. 10(a–d) are duplicated in Fig. 11(a–d), but the model incorporating moisture transfer was used to predict grain and exit air temperatures

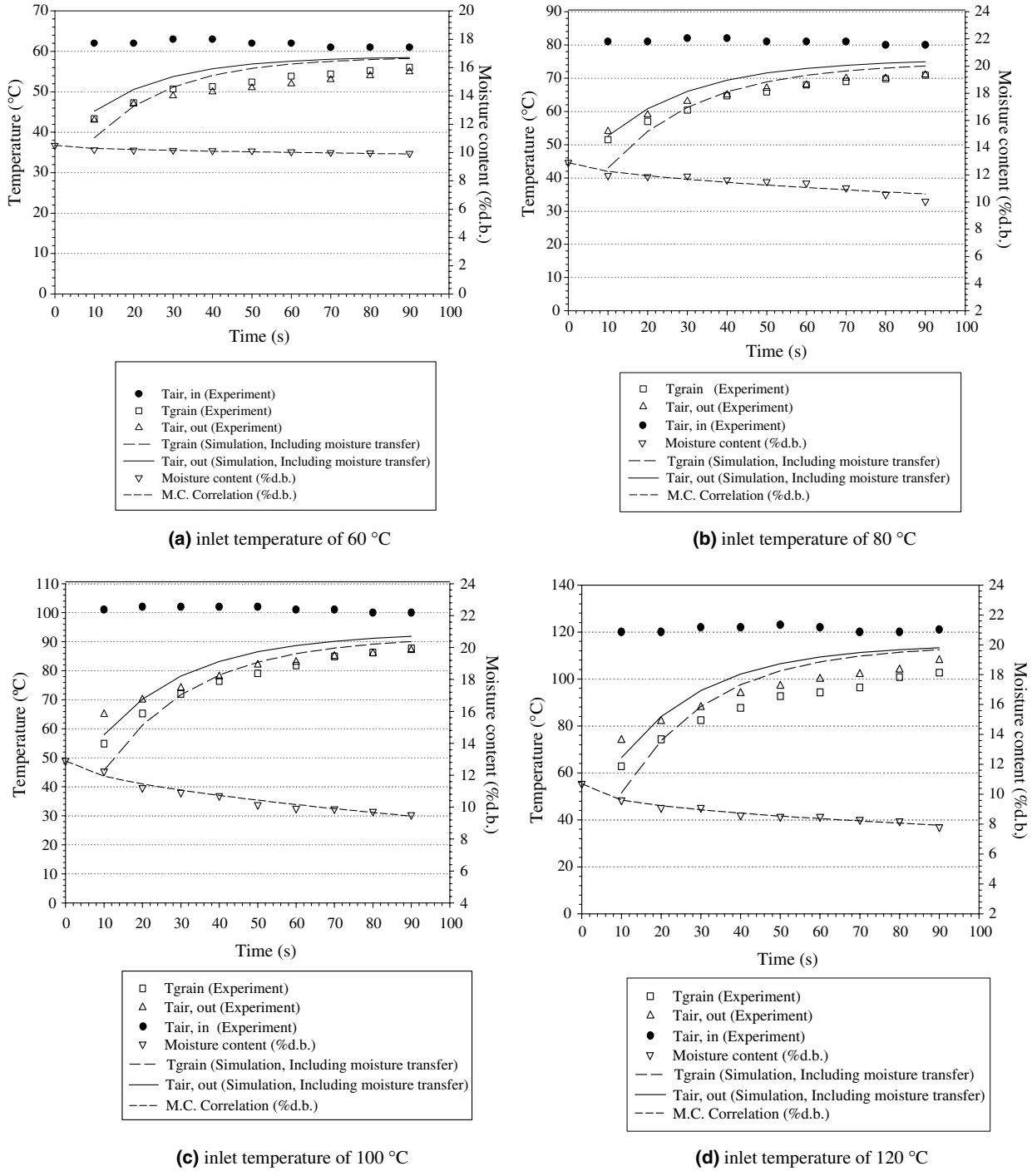

(a) inlet temperature of 60 °C

(b) inlet temperature of 80 °C

(c) inlet temperature of 100 °C

(d) inlet temperature of 120 °C

Fig. 11. Simulation and experimental results of heat disinfestation fluidized bed model coupling heat and mass transfer.

with a consequential improvement in predicted values. The model predicted grain temperature more accurately than exit air temperature, but not for the test undergoing inlet air temperature of 120 °C. The discrepancies between predicted and measured exit air temperatures are between 2 and 5 °C (except for the testing under high inlet air temperature of 120 °C) and may partly due to the effect of heat loss through the wall of the fluidized-bed chamber. The measuring point for the exit air is located 85 cm above the air distributor plate, which is quite high compared with a dynamic bed height where it is accompanied by most of the fluidized grain; hence, those temperature values represent the temperature of the air leaving the chamber rather than the temperature of the air leaving the bed.

The air temperature drop due to heat loss effect is reflected by consistently lower measured temperature of the air containing low energy, i.e. air with a low temperature of 60 °C than the measured temperature of the grain,

as presented in Fig. 11(a), which is not possible unless it is due to the heat loss effect. To investigate these errors, the hand calculations (not shown herein) were performed for heat loss calculation and found that the discrepancies may reduce to 0.5–2.5 °C instead of 2–5 °C if involving heat loss, confirming the responsibility of heat loss effect for these discrepancies, in part. The model performed reasonably well in predicting grain temperature, although the predicted values were over-estimated. The differences in predicted and measured values were less than 2–3 °C, except for conditions with high inlet air temperature of 120 °C. After thoroughly checking the model, we believed that the main factor significantly affecting grain temperature computation was the heat transfer coefficient. The heat transfer coefficient used in the model determined subject to the arithmetic mean temperature between the inlet and exit air, which may be not be an adequate representation of the temperature of the air across the bed. Some additional data were required to investigate the variation in air temperature along with the fluidized bed height. Measurements were taken and the data are shown in Fig. 12, which illustrates that the air temperature decreases sharply just above 2.5 cm from the air distributor plate and does not fall in temperature once it is about 10 cm above the air distributor plate. This means that the heat transfer coefficient, determined based on the arithmetic mean temperature of air is over-estimated, resulting in over-prediction of grain temperature. The effect of over-estimating the mean temperature of the air inside the bed will be more powerful, especially in high temperature conditions, e.g. air temperatures of 120 °C.

6.4. Model application for heat disinfestations

Although a long heat treatment time is adequate for us to be confident of destroying the insect population however, the period cannot be too long because it must be balanced with the impact on product quality. The appropriate lethal time required for the complete mortality of all insects embedded inside the product at various given operating conditions may be determined by simulating the time that all locations inside the product must attain the target temperature. Increasing the rate of mortality by allowing the product to undergo higher temperatures near the surface, and more rapidly promoting the target temperature at the center, or creating thermal shock [15,19,22], can also be simulated by the model.

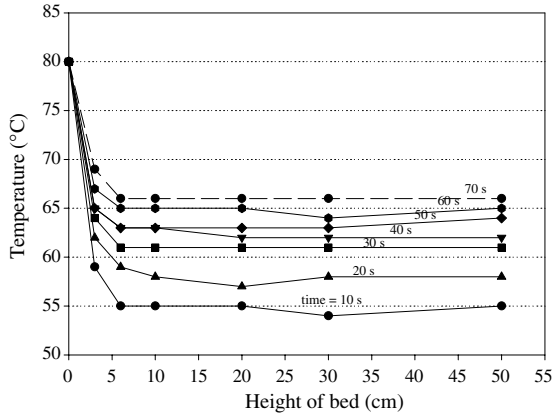

Fig. 12. Experimental results of variation of air temperature within the fluidized bed.

7. Conclusions

Cylindrical coordinates for the heat diffusion problem were chosen rather than spherical coordinates to model fluidized bed heat disinfestation because of its clearer picture of temperature profiles inside individual paddy kernels. The simulation results from the thin layer heat diffusion model, obtained from numerical methods, do not distinguish between those obtained from the analytical solution method and the numerical method was used in modeling. Coupling the thin-layer heat diffusion model with other relevant mass and energy balance equations that were developed for the relative parts of the fluidized bed system gave different results from applying the thin-layer model alone. It was quite apparent that only 1.0% d.b. of grain moisture reduction, the model which takes full account of the changes in energies due to differential changes in moisture content, significantly improve prediction of grain and exit temperatures. The model tends to over-estimate grain and exit temperatures in most cases considered, but the errors are not considered significant. The use of arithmetic mean temperature for air across the bed, to determine the heat transfer coefficient, was primarily motivated by the lack of information regarding variations in air temperature within the bed, and led to over-estimation of grain temperature, whilst the over-estimation of exit air temperature was mainly due to the heat loss effect. Finally, in applying heat disinfestations, the model is able to predict the mortality of insects inside grain kernels by knowing the lethal temperature and operating conditions, so that consequently the lethal time required for completely destroying all insects can be determined.

Acknowledgement

Thanks are due to the Thailand Research Fund (TRF) for financial support and the Japanese International Research Center for Agricultural Sciences (JIRCAS).

References

[1] J.L. Sharp, J.J. Gaffney, J.I. Moss, W.P. Gould, Hot-air treatment device for quarantine research, J. Econ. Entomol. 84 (1991) 520–527.
[2] L.G. Neven, Combined heat treatments and cold storage effects on mortality of fifth-instar codling moth (Lepidoptera: Tortricidae), J. Econ. Entomol. 87 (1994) 1262–1265.
[3] L.G. Neven, E.J. Mitcham, CATTS (controlled atmosphere/temperature treatment system): a novel tool for the development of quarantine treatments, J. Amer. Entomol. 42 (1996) 56–59.

[4] L.G. Neven, L.M. Rehfield, K.C. Shellie, Moist and vapor forced air treatment of apples and pears: effects on the mortality of fifth instar codling moth (Lepidoptera: Tortricidae), J. Econ. Entomol. 89 (1996) 700–704.
[5] S. Lurie, Postharvest heat treatments, Postharvest Biol. Technol. 14 (1998) 257–269.
[6] R.L. Mangan, K.C. Shellie, S.J. Ingle, M.J. Firko, High temperature forced-air treatments with fixed time for 'Dancy' tangerines, 'Valencia' orange and 'Rio Star' grape fruit, J. Econ. Entomol. 91 (1998) 933–939.
[7] K.K. Jacobi, L.S. Wong, J.E. Giles, Postharvest quality of zucchini (*Cucurbita pepo* L.) following high humidity hot air disinfestation treatments and cool stage, Postharvest Biol. Technol. 7 (1996) 309–316.
[8] N.W. Heather, R.J. Corcoran, R.A. Kopittke, Hot air disinfestation of Australian 'Kensington' mangoes against two fruit flies (Diptera: Tephritidae), Postharvest Biol. Technol. 10 (1997) 99–105.
[9] C.F. Hayes, H. Young, Extension of model to predict survival from heat transfer of papaya infested with oriental fruit flies (Diptera: Tephritidae), J. Econ. Entomol. 82 (1989) 1157–1160.
[10] J.D. Hansen, Heating curve models of quarantine treatments against insect pests, J. Econ. Entomol. 85 (1992) 1846–1854.
[11] S. Wang, J. Tang, R.P. Cavalieri, Modeling fruit internal heating rates for hot air and hot water treatment, Postharvest Biol. Technol. 22 (2001) 257–270.
[12] T. Dermott, D.E. Evans, An evaluation of fluidized-bed heating as a means of disinfesting wheat, J. Stored Prod. Res. 14 (1978) 1–12.
[13] D.E. Evans, T. Dermott, Dosage-mortality relationships for *Rhyzopertha dominica* (F.) (Coleoptera: Bostrychidae) exposed to heat in a fluidized bed, J. Stored Prod. Res. 17 (1981) 53–64.
[14] D.E. Evans, The influence of some biological and physical factors on the heat tolerance relationships for *Rhyzopertha dominica* (F.) and *Sitophilus oryzae* (L.) (Coleoptera: Bostrychidae and Curculationidae), J. Stored Prod. Res. 17 (1981) 65–72.
[15] D.E. Evans, The influence of rate of heating on the mortality of *Rhyzopertha dominica* (F.) (Coleoptera: Bostrychidae), J. Stored Prod. Res. 23 (1987) 73–77.
[16] D.E. Evans, G.R. Thorpe, T. Dermott, The disinfestation of wheat in a continuous-flow fluidized bed, J. Stored Prod. Res. 19 (1983) 125–137.
[17] G.R. Thorpe, The thermodynamic performance of a continuous-flow fluidized bed grain disinfestor and dryer, J. Agric. Eng. Res. 37 (1987) 27–41.
[18] J.K. Claflin, D.E. Evans, A.G. Fane, R.J. Hill, The thermal disinfestation of wheat in a spouted bed, J. Stored Prod. Res. 22 (1986) 153–161.
[19] S.J. Beckett, R. Morton, Mortality of *Rhyzopertha dominica* (F.) (Coleoptera: Bostrychidae) at grain temperatures ranging from 50 °C to 60 °C obtained at different rates of heating in a spouted bed, J. Stored Prod. Res. 39 (2003) 313–332.
[20] J.W. Sutherland, D.E. Evans, A.G. Fane, G.R. Thorpe, Disinfestation of grain with heated air, in: E. Donahaye, S. Navarro (Eds.), Proceeding of the Fourth International Working Conference on Stored-Product Protection, Tel Aviv, Israel, Maor-Wallach Press, Jerusalem, Israel, 1987, pp. 261–274.
[21] J.W. Sutherland, P.W. Fricke, R.J. Hill, The entomological and thermodynamic performance of a pneumatic conveyor wheat disinfestor using hot air, J. Agric. Eng. Res. 44 (1989) 113–124.
[22] H. Mourier, K.P. Poulsen, Control of insects and mites in grain using a high temperature/short time (HTST) technique, J. Stored Prod. Res. 36 (2000) 309–318.
[23] J.M. Vergnaud, Drying of Polymeric and Solid Materials: Modelling and Industrial Application, Springer-Verlag, London, 1992, pp. 13–70.
[24] M.N. Ozisik, Heat Transfer: A Basic Approach, McGraw-Hill, New York, 1985, pp. 124–127.
[25] F. Bowman, Introduction to Bessel Functions, Dover Publications, Inc., New York, 1958, pp. 1–3.
[26] D. Kunii, O. Levenspiel, Fluidization Engineering, second ed., Butterworth-Heinemann, Boston, 1991, Chapter 11, pp. 268–271.
[27] A.S. Mujumdar, Handbook of Industrial Drying, second ed., Marcel Dekker, Inc., New York, 1995. Appendix.
[28] D.B. Brooker, F.W. Bakker, C.W. Hall, Drying and Storage of Grain and Oilseed, AVI, New York, 1992. Appendix E.
[29] C. Laithong, Study of thermo-physical properties of rough rice, M.Sc. Thesis, King Mongkut's Institute of Technology Thonburi, Bangkok, Thailand, 1987.
[30] Z. Pakowski, Z. Bartezak, C. Strumillo, S. Stenstrom, Evaluation of equations approximating thermodynamic and transport properties of water, stream and air for use in CAD of drying processes, Drying Technol. 9 (3) (1991) 753–773.